Tether Length Control for Orbital Transfer of Tethered Satellite

Shinji Hokamoto, Naritoyo Shibata
Department of Aeronautics and Astronautics, Kyushu University
744 Motooka, Nishi-ku, Fukuoka 819-0395, Japan

This study discusses orbital transfer of a tethered satellite system in equatorial plane. By applying a nonlinear control method, this paper proposes a procedure to design a tether length profile which attains the designated states at a specified final position in orbit. The proposed procedure consisting of three steps adjusts the system's three states to the target values with one control input; control for the angular momentum of pitching motion, which leads to control of the tether length, control for the pitch angular rate, and control for the pitch angle. The proposed procedure does not require numerical iterations, and can cope with physical restrictions for the system, such as tether tension or the maximum tether length. Besides, the resulted final states are precisely coincident to the target values.

テザー長制御によるテザー衛星の軌道変換

外本　伸治，柴田　成豊
九州大学大学院工学研究院航空宇宙工学部門／九州大学大学院工学府航空宇宙工学専攻

本研究では，赤道面内におけるテザー衛星の軌道変換について研究する．非線形制御の手法を用いることにより，指定された軌道上位置でシステムの状態を所望の値にするテザー長の履歴を作成する方法を提案する．テザー長を制御することになるピッチ角運動量の制御，ピッチ角速度の制御，ピッチ角の制御，という 3 つのステップにより，1 つの入力で 3 つの状態を制御する．提案する手法は，数値反復計算を必要としないだけでなく，テザー張力などの物理的拘束にも対応できる．また，システムの状態を正確に目標値に一致させることができる．

1. Introduction

Control thruster forces are most commonly used for orbital transfer, but fuel consumption may become a critical problem. Thus, some works have discussed to utilize a gravity gradient force as an alternative force which does not consume propellant for orbital transfer.

Murakami[1] and Watanabe and Nakamura[2] discuss the gravity gradient effect on the attitude of 'rigid' satellites in circular orbits. Martinez-Sanchez and Gavit[3] and Landis[4] treat a dumbbell-type tether satellite, and investigate orbital perturbations for the tether extension / retrieval. However, all the above papers focus on control of one orbital element, and do not address other elements. Consequently, the orbit is controlled to one in an infinite set of orbits defined by the other orbital elements. In contrast, the reference [5] treats a rigid satellite with two control inputs, and addresses a problem to transfer the orbit into a prescribed one defined by three orbital elements.

All the above works utilize gravity gradient force as orbital transfer force directly. As a result, the orbital transfer effect is extremely small even for huge satellite systems, because gravity gradient force is much smaller than central force for orbital motion.

Ziegler and Cartmell[6] and Hoyt and Uphoff[7] have proposed the following orbital transfer concept for a dumbbell-type satellite system. Firstly, a gravity gradient force induces the pitching motion of the system to generate relative velocity increment of its end-point satellites. Subsequently, the system separates the end-point satellite when it has a desired velocity vector increment for orbital transfer.

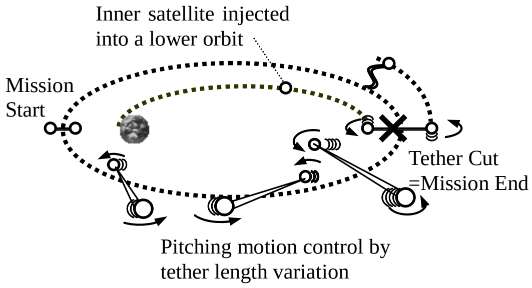

Fig.1 Mission outline for the orbital transfer.

This concept enables effective orbital transfer, because even small gravity gradient forces can generate non-small magnitude of relative velocity through the pitching motion of the satellite. However, they do not address how to form an input profile leading to a desired velocity increment at a prescribed position in orbit.

This study discusses orbital transfer of a tethered satellite system (TSS) in equatorial plane. Figure 1 depicts the mission outline considered in this study. The first task to achieve a desired orbital transfer is to define a final position in orbit and a velocity vector increment. Subsequently, the final states corresponding to the desired velocity vector are specified. Then, tether expansion / retrieval profile is designed to achieve the final states through inducing pitching motion. When the TSS reaches the final position with the prescribed states, cutting the tether injects a satellite into a desired orbit.

This paper proposes a design procedure of the tether length profile to achieve the final states at the designated position in orbit. Since the proposed procedure is not based on numerical iterations, it has some advantages: the computational cost is small, the final states are precisely coincident to the target ones, physical restrictions are directly coped with, such as tether tension or the maximum tether length.

2. Governing Equations

This study deals with co-planar motion of a TSS in an elliptic orbit in equatorial plane. To simplify the problem, the tether is modeled to be mass-less and have no elastic deformation, and the size of the two end-point satellites is negligible.

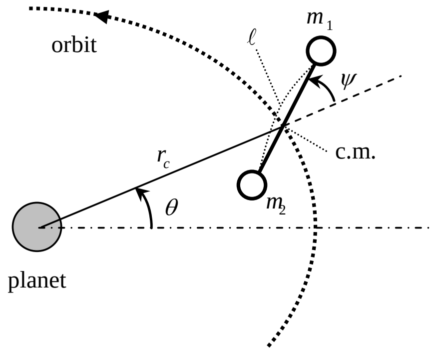

Fig.2 State variables of the TSS.

Figure 2 illustrates the principal variables of a TSS used in this study; θ indicates true anomaly, ψ pitch angle, ℓ tether length, r_c orbital radius, and m_i mass of the satellite i $(i = 1, 2)$. Applying Lagrange's equation to this system, the governing equation for the pitching motion is derived as follows.

$$\ddot{\psi} = -\ddot{\theta} - 3\frac{\mu}{r_c^3}\sin\psi\cos\psi - 2\frac{\dot{\ell}}{\ell}\left(\dot{\theta} + \dot{\psi}\right) \qquad (1)$$

where μ is a gravitational constant of the planet.

Although gravity gradient force perturbs the orbital motion of a TSS, the perturbation force is extremely small, because its magnitude is proportional to $\left(\ell / r_c\right)^2$. Thus, the orbital motion can be treated as a Keplerian motion. Hence the true anomaly θ has one-to-one mapping with time t, and time derivatives can be expressed by derivatives with respect to θ.

The system's angular momentum consists of two parts: one concerning its orbital motion and another its pitching motion. The latter angular momentum H_{pitch} is defined as the following equation.

$$H_{\text{pitch}} = \frac{m_1 m_2}{m_1 + m_2}\ell^2\left(\dot{\theta} + \dot{\psi}\right) \qquad (2)$$

Although the total angular momentum keeps constant when no external disturbance force exists, H_{pitch} can be changed by tether length variation according to its orbital motion.

Some mathematical manipulations derives from Eq.(2) the angular momentum change of the pitching motion in an orbital section $\left[\theta_A \;\; \theta_B\right]$ as follows.

$$\ln \frac{H_{\text{pitch}}(\theta_B)}{H_{\text{pitch}}(\theta_A)} = -\frac{3}{2}\int_{\theta_A}^{\theta_B} \frac{\sin 2\psi}{(1+e\cos\theta)(1+\psi')}\, d\theta \tag{3}$$

where the prime indicates the derivative with respect to θ. This equation implies several important notices: (1) for $\psi' = 0$, H_{pitch} increases (decreases) most effectively when $\psi = (3\pi)/4$ [rad] ($\pi/4$ [rad]), which is described in the references [1] and [2]; (2) when $|\psi'|$ is large enough, H_{pitch} keeps an almost constant value, because the integral is averaged for monotonous and rapid change of ψ; (3) variation of H_{pitch} depends not only on the length of control period but also on the orbital position in orbit, since the integral includes θ; (4) Eq.(3) is a nonholonomic constraint, because the integral has no closed-form solution.

3. Control Input Profile

To achieve a desired orbital transfer, the three state variables ($\ell, \psi, \dot{\psi}$) must be controlled to their target values at the final position in orbit. Even by applying nonholonomic control techniques, controlling three variables by one control input is not easy. Besides, Eq.(3) includes a time dependent variable θ explicitly, although typical problems with nonholonomic constraints do not. Therefore, finding a proper tether length profile for this system is categorized to a very difficult problem.

To solve the problem, this study takes an alternative input instead of the tether length. From Eq.(1), the rate of the tether length can be described as follows.

$$\frac{\dot{\ell}}{\ell} = \sqrt{\frac{\mu}{p^3}}(1+e\cos\theta)^2 \times\left\{-\frac{3}{4}\frac{\sin 2\psi}{(1+e\cos\theta)(1+\psi')} + \frac{e\sin\theta}{1+e\cos\theta} - \frac{1}{2}\frac{\psi''}{1+\psi'}\right\} \tag{4}$$

where p is the semi-latus rectum and e the eccentricity of the orbit.

This equation implies that once ψ'' profile is specified over an input section, the control input profile $\dot{\ell}$ over the section is also defined; the ψ'' profile designates the profiles of ψ' and ψ in the section, and hence all the variables in the right hand side are specified, and consequently they identify the input $\dot{\ell}$. The advantage of the alternative input is that adjusting ψ and ψ' at the end of the section becomes very easy.

The remained variable to control is the tether length ℓ. The second implication described after Eq.(3) gives a clue to adjust the variable. When the tether length ℓ is controlled so that H_{pitch} coincides to a value defined by the desired final $\ell, \dot{\psi}$ and $\dot{\theta}$, and when ψ' is controlled to its desired one keeping the desired H_{pitch}, ℓ also coincides to its desired value at the final position. It should be noted that the adjusting H_{pitch} must be conducted before the control of ψ and $\dot{\psi}$, because H_{pitch} keeps the desired value once $|\psi'|$ is large enough.

Consequently, the following three steps make the three state variables ($\ell, \psi, \dot{\psi}$) coincide to their desired ones.

Step 1: Coincide the pitch angular momentum H_{pitch} to a desired one defined for the final state.

Step 2: Adjust the pitch angular velocity $\dot{\psi}$ to the desired value.

Step 3: Adjust the pitch angle ψ to the desired value.

Each step can be accomplished by a tether length variation corresponding to a ψ'' profile explained below.

The following ψ'' profile composed of Fourier series bases in a section $[\theta_A \;\; \theta_B]$ gives a profile to satisfy the each step.

$$\psi''(\theta) = a_1 \sin\left(\frac{\theta-\theta_A}{\theta_B-\theta_A}\pi\right) + a_2 \sin\left(2\frac{\theta-\theta_A}{\theta_B-\theta_A}\pi\right) \tag{5}$$

After this input section, the profile generates the variations for its pitch angular velocity and pitch angle as follows.

$$\Delta\psi' = 2a_1 \frac{\theta_B - \theta_A}{\pi} \tag{6}$$

$$\Delta\psi = a_1 \frac{\left(\theta_B - \theta_A\right)^2}{\pi} + a_2 \frac{\left(\theta_B - \theta_A\right)^2}{2\pi} + \left(\theta_B - \theta_A\right)\psi'\left(\theta_A\right) \tag{7}$$

Thus, these variations specify the Fourier coefficients a_1 and a_2 to achieve the designated ψ and $\dot{\psi}$ in each step.

The first period in Step 1 changes the pitch angle ψ into $(3\pi)/4$ [rad] ($\pi/4$ [rad]) to increase (decrease) the pitching angular momentum most effectively. Besides, the target angular velocity $\dot{\psi}$ after the first period is set to be zero to keep the attitude. Then, the target states are specified in Step 1 as $\Delta\psi = \Delta\dot{\psi} = 0$ to keep the pitch angle until the H_{pitch} coincides to the desired value.

Step 2 uses only the coefficient a_1 to adjust the pitch angular velocity at the final state, i.e. $a_2 = 0$. It should be noted that the rotational motion must be hasten in an early period in Step 2 by retrieving the tether not to change the H_{pitch} adjusted in Step 1. Step 3 following Step 2 adjusts the pitch angle at the final state according to the proper $\Delta\psi$ and $\Delta\dot{\psi} = 0$.

4. Tether Tension

Pitching motion control by tether length variation needs to keep the tether tension positive. Especially in Step 1, the tether tension becomes easily negative, because the tether extends itself to keep the attitude in gravity gradient field.

The tether tension F_T can be also derived through Lagrange's procedure as follows.

$$F_T = \frac{m_1 m_2}{m_1 + m_2}\left[-\ddot{\ell} + \ell\left\{\left(\dot{\theta} + \dot{\psi}\right)^2 - \frac{\mu}{r_c^3}\left(1 - 3\cos^2\psi\right)\right\}\right] \tag{8}$$

A constraint of the tether tension $F_T \geq F_{T_{\min}}$, where $F_{T_{\min}}$ means an allowable minimum tension, can be arranged in the following expression:

$$\begin{aligned}\frac{\psi'''}{1+\psi'} \geq{} & \left(\frac{\psi''}{1+\psi'}\right)^2 + 2\left(\frac{\ell'}{\ell}\right)^2 + \left(\frac{H_{\text{pitch}}{}'}{H_{\text{pitch}}}\right)' \\ & + 2\frac{e\left(e+\cos\theta\right)}{\left(1+e\cos\theta\right)^2} - 4\frac{e\sin\theta}{1+e\cos\theta}\frac{\ell'}{\ell} \\ & - 2\left(1+\psi'\right)^2 + 2\frac{1-3\cos^2\psi}{1+e\cos\theta} \\ & + 2\frac{F_{T_{\min}}}{\dfrac{m_1 m_2}{m_1+m_2}\dfrac{\mu}{p^3}\ell\left(1+e\cos\theta\right)^4}\end{aligned} \tag{9}$$

where

$$\begin{aligned}\frac{\ell'}{\ell} = {} & -\frac{3}{4}\frac{\sin 2\psi}{\left(1+e\cos\theta\right)\left(1+\psi'\right)} - \frac{1}{2}\frac{\psi''}{1+\psi'} \\ & - \frac{e\sin\theta}{1+e\cos\theta}\end{aligned}$$

$$\begin{aligned}\left(\frac{H_{\text{pitch}}{}'}{H_{\text{pitch}}}\right)' = {} & -\frac{3}{2}\frac{\sin 2\psi}{\left(1+e\cos\theta\right)\left(1+\psi'\right)} \\ & \times\left(\frac{2\psi'\cos 2\psi}{\sin 2\psi} + \frac{e\sin\theta}{1+e\cos\theta} - \frac{\psi''}{1+\psi'}\right)\end{aligned}$$

Eq.(9) implies the following. Once the ψ'' profile is designed according to the design procedure explained in the previous section, ψ''' is also specified as well as ψ and ψ'. Thus, the remaining design parameter in Eq.(9) is only θ. Therefore, the period's length and position in orbit for Step 1 must be selected properly to guarantee positive tether tension. In steps 2 and 3, rapid rotational motion makes the tether tension positive.

5. Simulation Results

This section applies the proposed procedure for an orbital transfer problem and verifies the effectiveness.

As an example, this paper deals with a mission that a TSS in GTO injects a satellite into a LEO. The GTO is defined by $e = 0.7268$ and that the periapsis altitude is 300 [km]. The satellites' mass are $m_1 = m_2 = 25$ [kg], and the TSS has the following initial states at periapsis: $\ell(0) = 1$ [km], $\psi(0) = 0$ [rad], and $\dot{\psi}(0) = 0$ [rad/s]. It is assumed that a velocity vector increment required

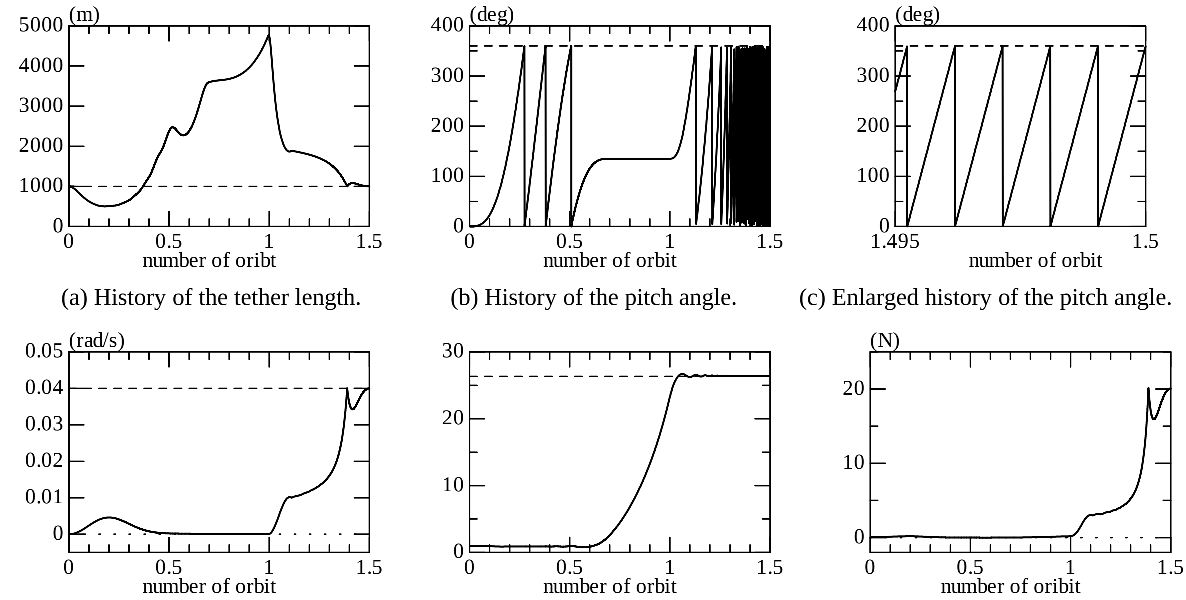

(a) History of the tether length. (b) History of the pitch angle. (c) Enlarged history of the pitch angle.

(d) History of the pitch angular velocity. (e) History of the angular momentum ratio. (f) History of the tether tension.

Fig.3 Simulation result 1 for an orbital transfer.

for the mission has already solved as $\Delta v = -20$ [m/s] in the circumferential direction at the apoapsis in the GTO.

The first simulation designates the final states as $\ell_f = 1$ [km], $\psi_f = 2n_1\pi$ [rad], and $\dot{\psi}_f = 0.04$ [rad/s] at $\theta_f = (2n_2 - 1)\pi$ [rad], where n_i indicates a natural number. Although the mission period becomes minimum when $n_2 = 1$, the tether tension becomes negative in Step 1. Thus this simulation takes $n_2 = 2$.

Figure 3 shows the simulation result. Figures (a) to (f) represent the time histories of tether length, pitch angle, pitch angle enlarged in the last section, pitch angular velocity, ratio of pitch angular momentum, and tether tension. The lateral axis in each figure indicates the number of orbit, i.e. $\theta/(2\pi)$, and each step period for the proposed procedure is allotted to the following number of orbit: the first period of Step 1 is $0 \sim 0.69$ and Step 1 ends at 0.995; Step 2 $0.995 \sim 1.11$; and Step 3 $1.11 \sim 1.50$. The target pitch angle at the end of the first period of Step 1 has been set to $(2\pi) \times 3 + (3\pi)/4$ [rad] to avoid negative tether tension (see figure (b)). The broken lines in the figures from (a) to (e) show the target value for the variables. The result indicates that the proposed design procedure precisely accomplishes the desired final states and works quite effective: the maximum tether length is less than 5 [km]. It should be noted that the tether tension depicted in the figure (e) keeps positive, although it is closed to zero in Step 1 (minimum value is 0.0011 [N]).

For a real orbital transfer, mission designers should take into considerations the following factors: (1) deciding separation point in orbit, (2) specifying velocity vector increment, and (3) designating target final states.

The second simulation compares the results according to the different final states. The simulation conditions are same as the previous one except the final tether length and angular velocity. Figure 4 shows the profiles of the tether length and tether tension for different final tether lengths. All cases have the same velocity vector increment $\Delta v = -20$ [m/s] at the apocenter. From these results, designing a longer tether length at the final point reduces the maximum tether tension, although it elongate the maximum tether length.

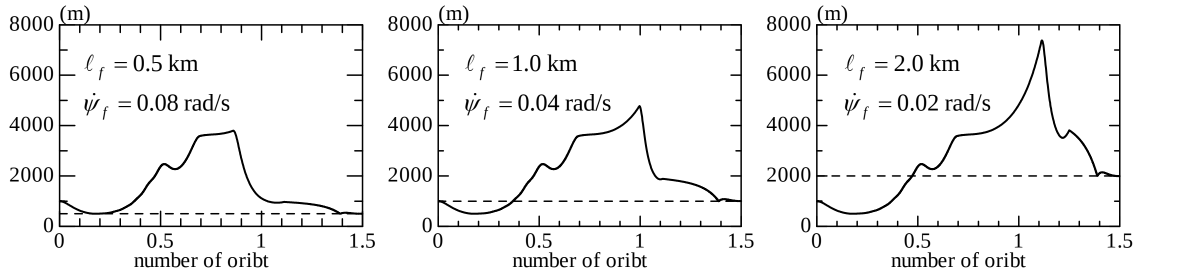

(a) History of the tether length (Case1). (b) History of the tether length (Case2). (c) History of the tether length (Case3).

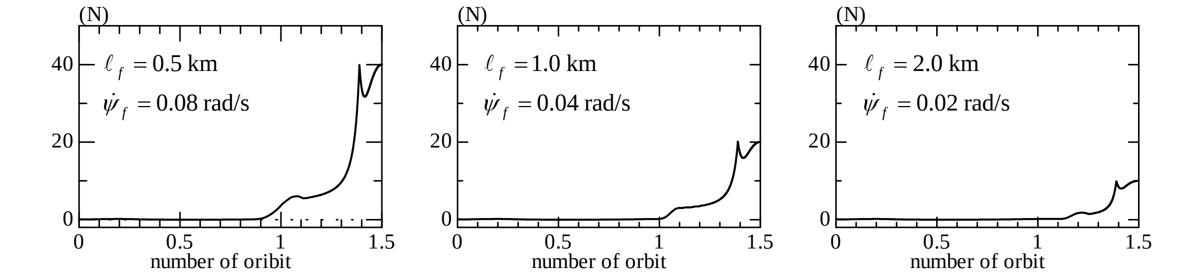

(d) History of the tether tension (Case1). (e) History of the tether tension (Case2). (f) History of the tether tension (Case3).

Fig.4 Simulation result 2 for different final states.

6. Conclusion

This study utilizes a tethered satellite system for orbital transfer of a satellite without thrusters. This paper proposes a design procedure of the tether length profile to achieve the final states at the designated position in orbit. The proposed procedure has some advantages: the computational cost is small, the final states are precisely coincident to the target ones, physical restrictions are directly coped with, such as tether tension or the maximum tether length.

References

[1] Murakami, C., "On Orbit Control Using Gravity Gradient Effect," Acta Astronautica, Vol.8, No.7, 1981, pp.733-747.

[2] Watanabe, Y. and Nakamura, Y., "Orbital Transfer of a Space System Using Gravity-Gradient," Proc. of 7th Workshop on Astrodynamics and Flight Mechanics, 1997, pp.44-49.

[3] Martinez-Sanchez, M. and Gavit, S.A., "Orbital Modifications Using Forced Tether-Length Variations," Journal of Guidance, Control, and Dynamics, Vol.10, No.3, 1987, pp.233-241.

[4] Landis, G.A., "Reactionless Orbital Propulsion Using Tether Deployment," Acta Astronautica, Vol.26, No.5, 1992, pp.307-312.

[5] Hokamoto, S., "Orbital Control of Satellite System Using Nonholonomic Control Theory, " Proceedings of the AIAA/AAS Astrodynamics Specialist Conference, Paper No. AAS-05-348, 2005

[6] Ziegler, S. W. and Cartmell M. P., "Using Motorized Tethers for Payload Orbital Transfer," Journal of Spacecraft and Rockets, Vol.38, No.6 (2001), pp.904-913.

[7] Hoyt, R. P., and Uphoff C., "Cislunar Tether Transport System," Proc. of the 35th AIAA/ASME/SAE/ASEE Joint Propulsion Conference, Paper No. AIAA-99-2690.